



THE INFLUENCE OF LARGE DEFORMATIONS OF ELASTOMERIC BEARINGS

1

Davide FORCELLINI¹ and James Marshall KELLY²

ABSTRACT

Seismic isolation using multi-layer elastomeric isolators has been used in the United States for more than 20 years. Although isolation bearings normally have a large factor of safety against buckling due to low shear stiffness, this phenomenon has been widely studied. In particular, the adopted linearly elastic theory is relatively accurate and adequate for most design purposes. Unfortunately it cannot consider the large deformation response of a bearing when buckling occurs and the unresolved behaviour of the stability of the post-buckled state. The study conducted in this paper may be viewed as a development of the linear theory of multi-layered elastomeric bearing, simply replacing the differential equations by algebraic equations, showing how it is possible to evaluate the post-buckling behaviour and the interactions at large deformations.

INTRODUCTION

Multilayered elastomeric bearings are very widely used in civil engineering as vibration mounts, bridge bearings and as seismic isolators for buildings. In these examples the bearing is in compression with in some cases the presence of shear. In other cases, such as tall buildings in near-fault locations seismic code requirements can lead to situations where some bearings in an isolation system can be required to take tension. The axial load effects investigated with experimental tests (such as Buckle et al., 2002, Han et al., 2013 and Sanchez et al., 2013) or with numerical simulations (such as Nagarajaiah and Ferrel, 1999, Warn and Weisman, 2011 and Weisman and Warn, 2012), can be explained by a simplified two-spring model of the bearing (Kelly, 1997). This theory can take into consideration the buckling response using an explicit force–deformation relation while maintaining a direct physical understanding of the phenomenon.

This paper is aimed to study the response of this model retaining the large deformation kinematics and comparing the response to stable and unstable post-buckling beam behaviour. It will also be used to illustrate the influence of large deformations on the various interactions between horizontal stiffness and vertical load and between vertical stiffness and horizontal displacement.

¹ Dr., Dept. of Civil Engineering, Univ. of San Marino, San Marino, davide.forcellini@unism.sm

² Pr. Em., Pacific Earthquake Engineering Research (PEER) Center, University of California at Berkeley, Richmond, CA, 94804-4698, jmkelly@berkeley.edu

STATE OF THE ART

Multilayered elastomeric bearings can be susceptible to a buckling type of instability similar to that of an ordinary column, but dominated by the low shear stiffness of a bearing. This phenomenon can be studied by a buckling analysis that treats the bearing as a continuous system considering the bearing to be a beam with the deformation assumed to be such that plane sections normal to the undeformed central axis remain plane, but not necessarily normal to the deformed axis. This theory of buckling in isolation bearings is an outgrowth of work by Haringx (1948) on the mechanical characteristics of helical steel springs and rubber rods used for vibration mountings. This work was published in a series of reports, the third of which Haringx (1948) covers the stability of solid rubber rods.

The Haringx theory was later applied by Gent (1964) to the problem of the stability of multilayered rubber compression springs and this application forms the basis for the theory of buckling in elastomeric isolators. The axial load effects described in such theories can be explained by a simplified two-spring model of the bearing (Kelly, 1997) that can take into consideration these effects using explicit force–deformation relations while maintaining the direct physical understanding of the phenomenon.

THE LINEAR TWO SPRING MODEL

Although this simple linear two-spring model accurately reflects the mechanical features of the linear theory of the multilayer elastomeric isolator, it does not make any predictions about the post-buckling behaviour or about the influence of large deformation geometry. Replacing differential equations by algebraic equations allows these effects to be included and to reveal the post-buckling behaviour and the interactions at large deformations.

The linearized form of the two-spring model leads to a characteristic equation for the buckling load in the form

$$P^2 + P \cdot P_S - P_S \cdot P_E = 0 \quad (1)$$

where

$P_E = \frac{\pi EI_s}{h^2}$ is the Euler load for a standard column with bending stiffness EI_s and height h ,

P_s is the shear stiffness of a unit element of an isolator denoted by GA_s .

For a circular bearing with radius R , total rubber thickness t_r and shear modulus G these become:

$$EI_s = \frac{1}{3} (6GS)^2 I \frac{h}{t_r}$$

$$\text{and } GA_s = GA \frac{h}{t_r}$$

where S is the shape factor for an individual layer of the bearing.

The shape factor of a typical isolator tends to be greater than 10 and less than 30 so that the important parameter denoted here by λ and defined by:

$$\lambda^2 = \frac{P_s}{P_E} \quad (2)$$

tends to be very small, usually of the order of 0.05 to 0.001.

The predicted critical loads are

$$P_{crit} = -\frac{P_s}{2} + \sqrt{\frac{P_s^2}{4} + P_s \cdot P_E} \quad (3)$$

and

$$T_{crit} = \frac{P_s}{2} + \sqrt{\frac{P_s^2}{4} + P_s \cdot P_E} \quad (4)$$

Normalizing these by dividing by $\sqrt{P_s \cdot P_E}$, gives:

$$p_{crit} = \frac{P_{crit}}{\sqrt{P_s \cdot P_E}} = -\frac{\lambda}{2} + \sqrt{\left(1 + \frac{\lambda^2}{4}\right)} \quad (5)$$

and

$$t_{crit} = \frac{T_{crit}}{\sqrt{P_s \cdot P_E}} = \frac{\lambda}{2} + \sqrt{\left(1 + \frac{\lambda^2}{4}\right)} \quad (6)$$

which by binomial expansion is

$$p_{crit} = 1 - \frac{\lambda}{2} + \frac{\lambda^2}{2} \quad (7)$$

and

$$p_{crit} = 1 + \frac{\lambda}{2} + \frac{\lambda^2}{2} \quad (8)$$

showing that the tensile critical load is slightly higher than the compression buckling load (by λ) and that they can both be approximated to high degree of accuracy by $\sqrt{P_s \cdot P_E}$.

It is unexpected that the buckling analysis for compression predicts that the isolator can buckle in tension at a load close to that for buckling in compression. There are many examples of strange systems that buckle in tension but these are entirely pathological in that the tension forces are always transferred to compression elements that produce the instability. This is not the case here. The buckling process really is tensile. The linear elastic model that leads to both compression and tension buckling is an extremely simple one and it might be argued that the tensile buckling may be an artifact of the model itself and not of the isolator. To show that this is not the case, a numerical simulation using a finite element model of a multi-layer elastomeric bearing was done and revealed that the prediction of tensile buckling by the simple linear elastic theory is in fact accurate and not an artifact of the model. For more details, see Kelly et al. (2007) and Forcellini and Kelly (2014). The essential point is that the mechanics of the isolator in tension are the mirror image of those for the isolator in compression. In particular, when the isolator is in compression below the buckling load but laterally displaced, the layers in the center experience rotations that give the vertical load a component along the layer causing a shear deformation. In tension, the layers in the center experience rotations in the opposite direction giving a shear deformation due to the tensile force that permits the top of the isolator to move upwards by a much larger displacement than that which could be sustained in pure tension with no lateral displacement. The simple two-spring model is used in the paper to help understand this somewhat unexpected result.

LARGE DEFORMATION OF THE TWO-SPRING MODEL

The large deformation response of the multilayer elastomeric isolator is shown by the simple two-spring model (shown in Figure 1) that takes into consideration both the bending and the shear behaviour of the isolator and which has been used to give convenient solutions for many aspects of the response of these bearings under the assumptions of linearized deformation kinematics. In the model two rigid elements in the shape of tees are connected by moment springs across hinges at top and bottom and by shear springs and frictionless rollers at mid-height. The two deformation variables shown are shear displacement, s , and relative rotation, θ . The two moment spring stiffness are shown as $\frac{1}{2} K_1$ each (moment/radian), the shear spring stiffness as K_2 (shear force/displacement), the vertical load as P , and the horizontal load at the top of the column as F_H .

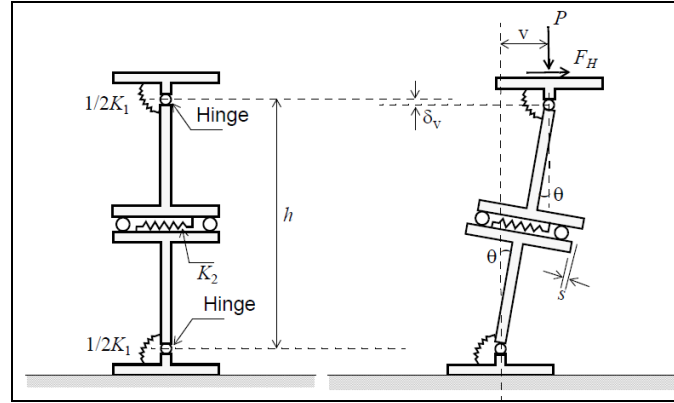


Figure 1. Two-spring model representing bearing response used to take into consideration both the bending and the shear behaviour of the isolator (Kelly, 1997)

To relate the quantities of this system to those of the continuous beam theory, we recognize that if the shear stiffness (K_2) is set to infinity, the buckling load of the model is K_1/h . On the other hand, if the rotational spring stiffness (K_1) is infinite and only shear deformation is allowed, the horizontal stiffness is $K_2 \cdot h$.

It follows that K_1 should be equated to $P_E \cdot h$ and K_2 to P_s/h , where P_E is the Euler buckling load of the column neglecting shear deformation, and P_s is the effective shear of the bearing.

In the stability analysis of multilayer bearings (Koh and Kelly, 1986 and Kelly, 1997), the bearing is treated as a continuous composite system in which the steel layers do not deform, allowing prediction of the buckling load and the effective lateral stiffness in the presence of axial load. The stability theory resembles the linearized theory of an elastic column, but accounts for shear deformation by considering rotation of the cross section, which is independent of the lateral deflection (Koh and Kelly, 1986). Also predicted by stability analysis (Koh and Kelly, 1986), the multilayer bearing under simultaneous lateral and axial loading undergoes an additional vertical displacement beyond that due to material axial flexibility. In these cases, the simplified Linear Two-Spring Model (Kelly, 1997) can take into considerations the preceding effects using explicit force–deformation relations.

When the assumption of large deformations is considered, the kinematic variables of the top of the column in terms of s and θ are:

the horizontal displacement of the top of the column:

$$v = h \cdot \sin \theta + s \cdot \cos \theta \quad (9)$$

the vertical displacement:

$$d = \delta_v = s \cdot \sin \theta + (1 - \cos \theta) \cdot h \quad (10)$$

The equilibrium equations are:

$$P \cdot v + h \cdot F_H \cdot \cos \theta = P_E \cdot h \cdot \theta \quad (11)$$

$$P \cdot \sin \theta + F_H \cdot \cos \theta = P_s \cdot \frac{s}{h} \quad (12)$$

Solving equation (12) for s/h:

$$\frac{s}{h} = \frac{P}{P_s} \cdot \sin \theta + \frac{F_H}{P_s} \cdot \cos \theta \quad (13)$$

substituting (9) and (13) into (11) and dividing by h, it gives:

$$P \cdot \sin \theta + P \cdot \left(\frac{P}{P_s} \sin \theta + \frac{F_H}{P_s} \cos \theta \right) \cdot \cos \theta + F_H \cdot \cos \theta = P_E \cdot \theta \quad (14)$$

Normalizing the specified loads P and F_H using $\sqrt{P_s \cdot P_E}$, leads to:

$$p = \frac{P}{\sqrt{P_s \cdot P_E}} \quad (15)$$

$$f = \frac{F_H}{\sqrt{P_s \cdot P_E}} \quad (16)$$

Dividing (14) by h and introducing (15) and (16) in (12) becomes:

$$p \sqrt{P_E P_s} \cdot \sin \theta + p \sqrt{P_E P_s} \cdot \left(\frac{p \sqrt{P_E P_s}}{P_s} \sin \theta + \frac{f \sqrt{P_E P_s}}{P_s} \cos \theta \right) \cdot \cos \theta + f \sqrt{P_E P_s} \cos \theta = P_E \theta \quad (17)$$

Dividing Equation (17) by $\sqrt{P_s \cdot P_E}$, it is possible to obtain:

$$p \cdot \sin \theta + p \cdot \left(p \cdot \frac{1}{\lambda} \cdot \sin \theta + f \cdot \frac{1}{\lambda} \cdot \cos \theta \right) \cdot \cos \theta + f \cos \theta = \frac{1}{\lambda} \cdot \theta \quad (18)$$

and this can be rewritten in a compact way:

$$(p \cdot \cos \theta + \lambda) \cdot (p \cdot \sin \theta + f \cos \theta) = \theta \quad (19)$$

Finally, Eqs. (13), (9) and (10) can be rewritten as:

$$\frac{s}{h} = \frac{1}{\lambda} \cdot (p \cdot \sin \theta + f \cos \theta) \quad (20)$$

$$\frac{v}{h} = \sin \theta + \frac{1}{\lambda} \cdot (p \cdot \sin \theta + f \cos \theta) \quad (21)$$

$$\frac{\delta_v}{h} = \frac{s}{h} \sin \theta + 1 - \cos \theta \quad (22)$$

Equations (19), (20), (21) and (22) define the kinematics solution of the problem. The method of solution is to fix λ and p and solve for f as a function of θ and then calculate the other quantities as functions of θ and plot in terms of f .

Figure 2 represents the solution of Eq. 4.9 for several values of p . Figure 3 - Figure 5 show the results for the quantities $(s/h, v/h, \delta_v/h)$ in terms of the large kinematics.

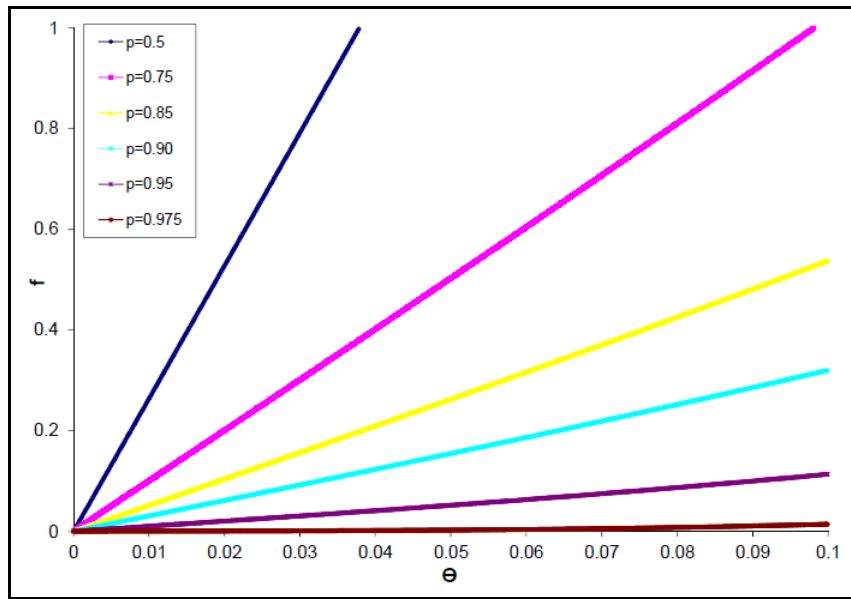


Figure 2. Eq. 19 representation

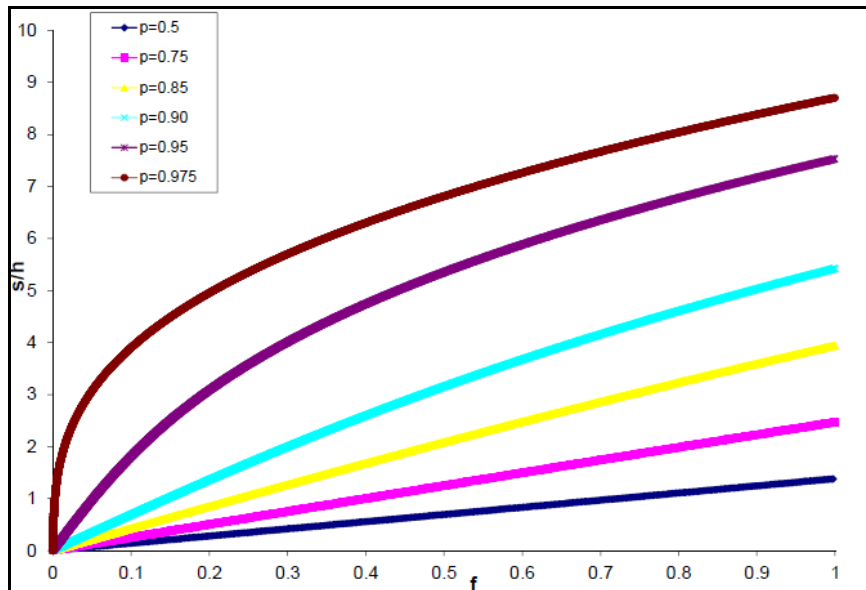


Figure 3. s/h-f representation

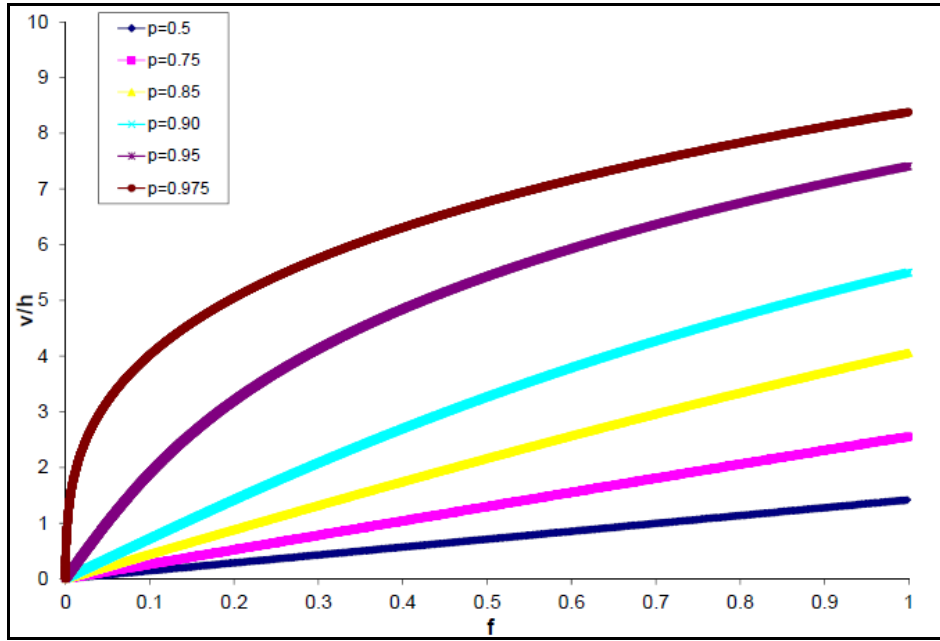


Figure 4. v/h - f representation

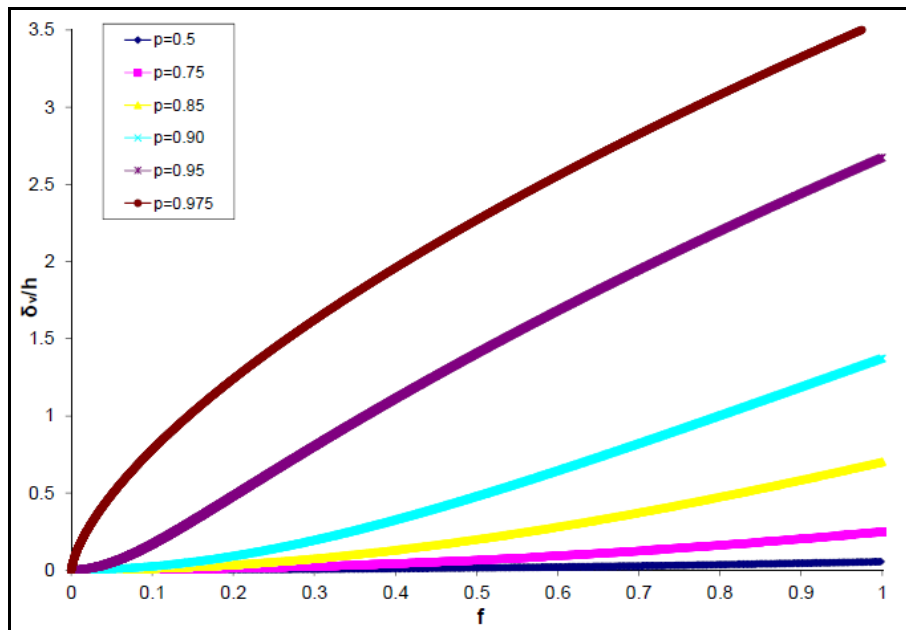


Figure 5. δ_v/h - f Representation

LARGE DEFORMATION KINEMATICS WITH VERTICAL TENSILE LOAD

The theoretical formulation seen in the previous section can be applied in the case of vertical tensile loads. In particular, the two-spring model and its kinematics are shown in Figure 6, where the loads at the top of the column are defined as $T = -P$ for the vertical load and F_H for the horizontal load. Figure 7 represents the solution for several values of t . Figure 8 - Figure 10 show the results for the quantities $(s/h, v/h, \delta_v/h)$ in terms of the large kinematics.

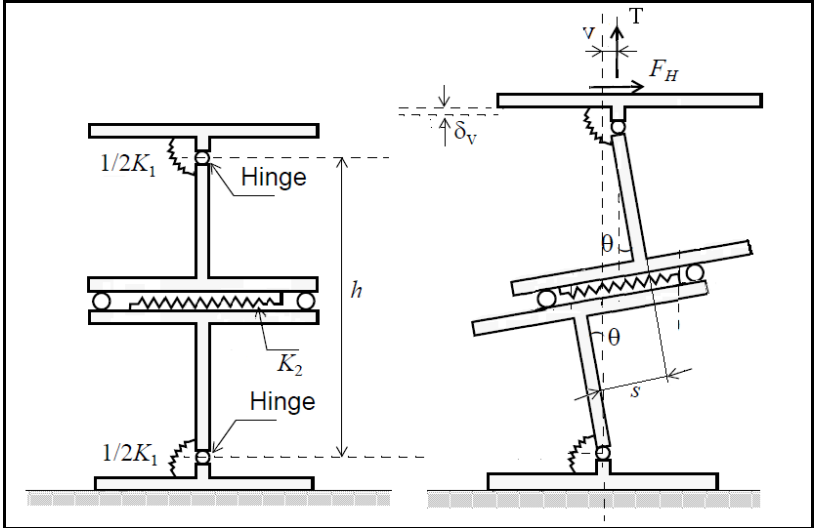


Figure 6. Deformation of the Two-spring Model with Tensile Load

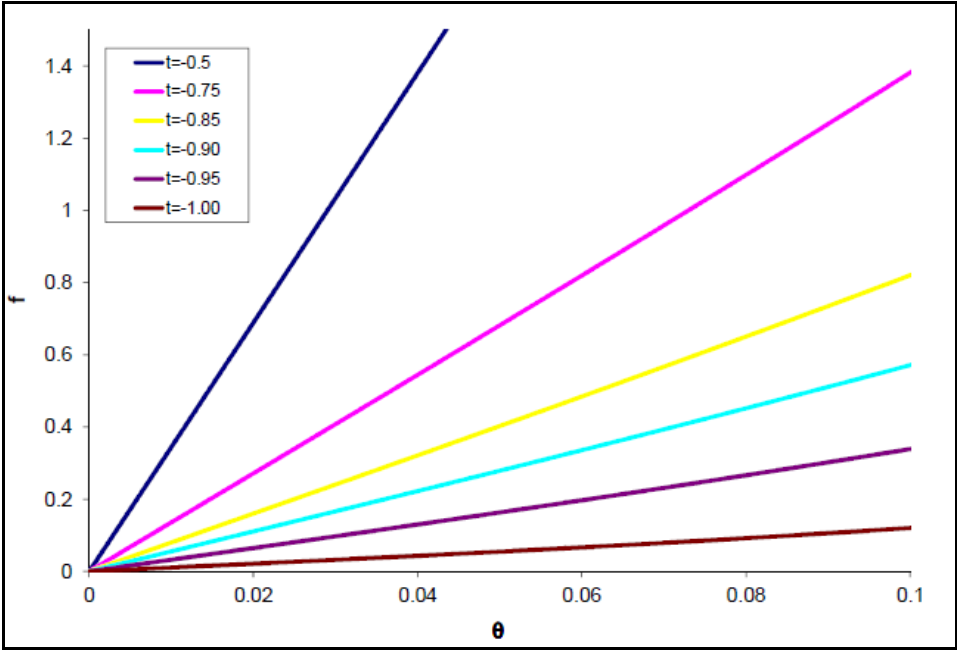


Figure 7. Eq. 9 Representation

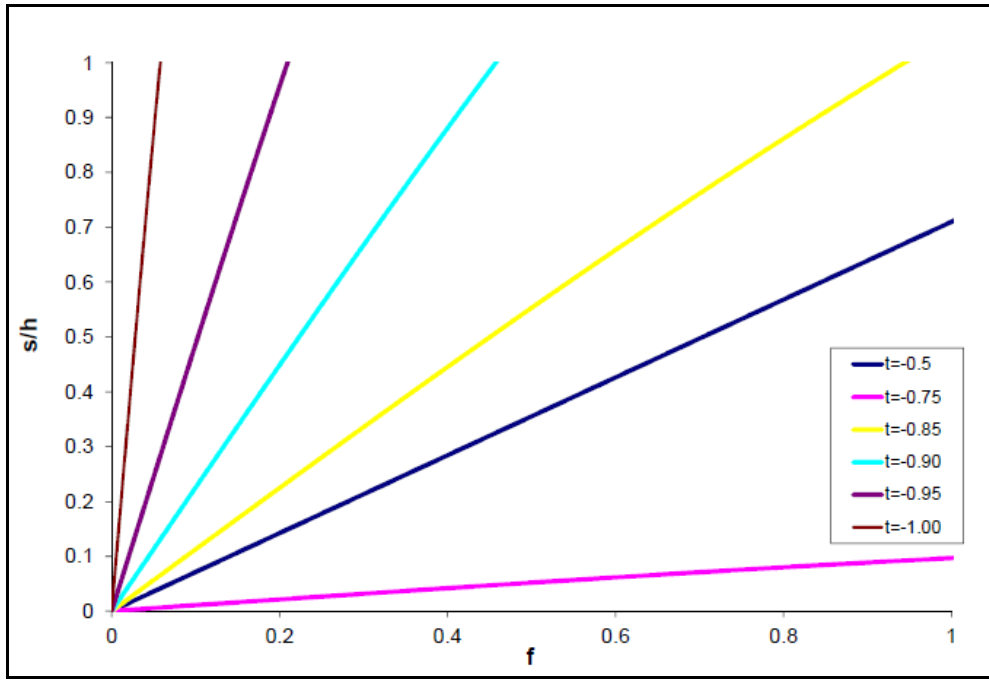


Figure 8. $s/h - f$ Representation

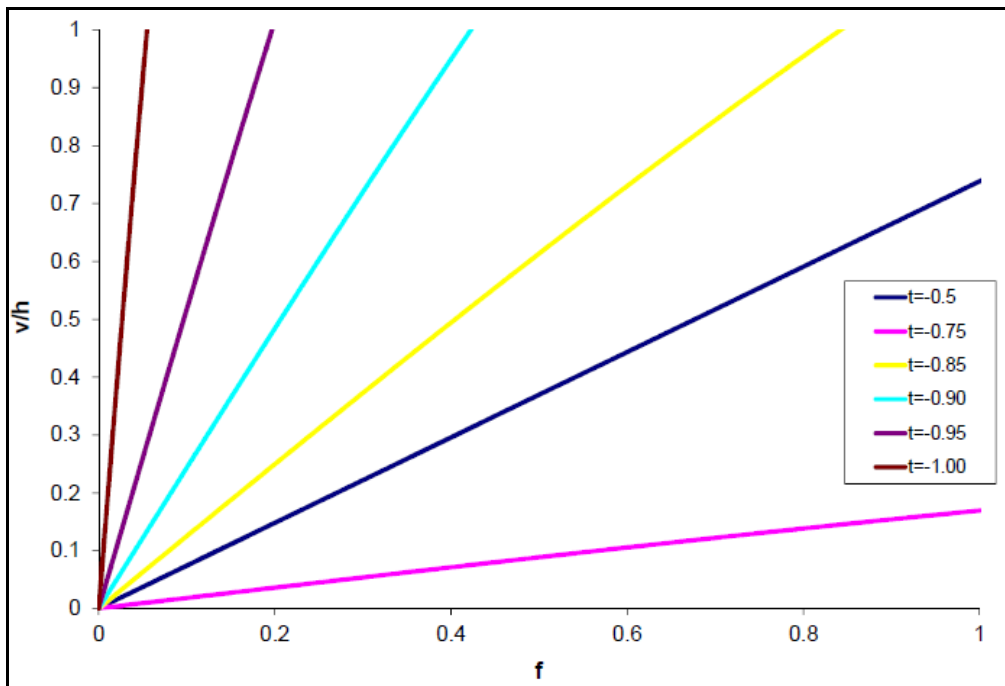


Figure 9. $v/h - f$ Representation

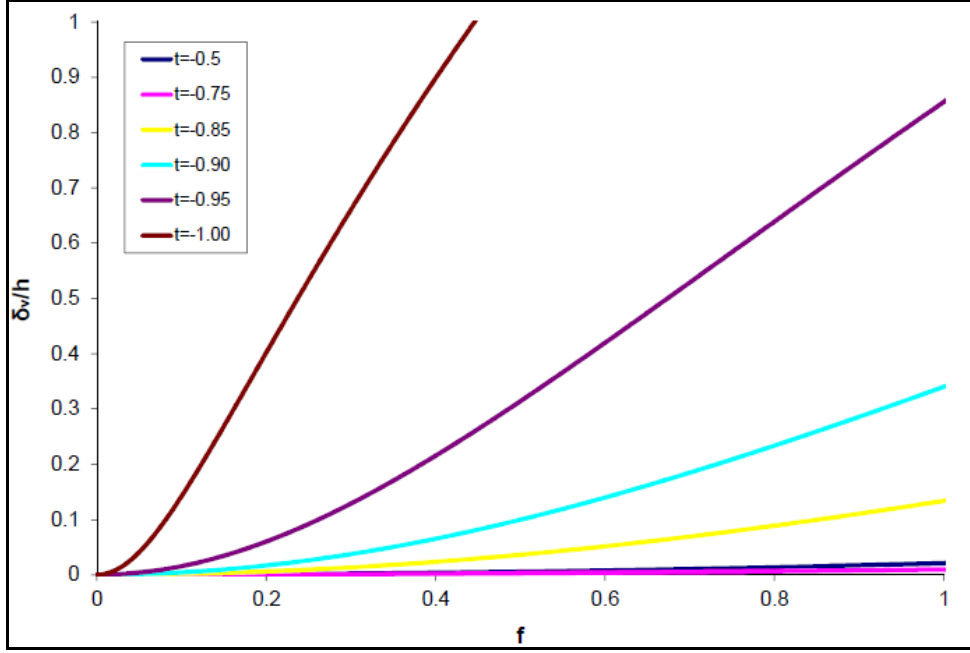


Figure 10. δ_v/h - f Representation

BUCKLING AND POST-BUCKLING IN TWO-SPRING MODEL

In a way that is quite similar to the study of the post-buckling behavior of continuous columns illustrating both stable and unstable response, by looking at the response of the model when imperfections are present, either from fabrication or from geometric and material variations, a theory can be derived from the simple two-spring model in which all the imperfections are condensed into an initial θ_0 angle.

The two-spring model (Figure 1) is then defined by the following equilibrium equations:

$$P \cdot v = P_E \cdot h \cdot (\theta - \theta_0) \quad (23)$$

$$P \cdot \sin \theta = P_S \cdot \frac{s}{h} \quad (24)$$

Considering the assumption of large deformations, the kinematics variables of the top of the column in terms of s and θ are still:

$$\frac{v}{h} = \sin \theta + \frac{s}{h} \cdot \cos \theta \quad (25)$$

Substituting Eqs. (24) and (25) into Eq. (23) and dividing by h , gives the quadratic equation:

$$P^2 \cdot \frac{\cos \theta \cdot \sin \theta}{P_S} + P \cdot \sin \theta - P_E \cdot (\theta - \theta_0) = 0 \quad (26)$$

which will provide two solutions. The positive solution gives results in the compression (Figure 11) and the negative in tension (Figure 12) for various values of θ_0 angle. These figures show that the post-buckling behaviors in compression and tension are both stable.

In practice, this may not be the case for the real isolator since the rubber is not truly linear and might soften with increasing shear strain. However most natural rubber compounds tend to stiffen with increasing strains beyond a shear strain of around 150% due the effect called strain crystallization and this will lead to an increasing vertical load and the restoration of stability. It is not possible to demonstrate this by the simple model since there is not really a measure of shear strain in the model. This could be object of further investigations.

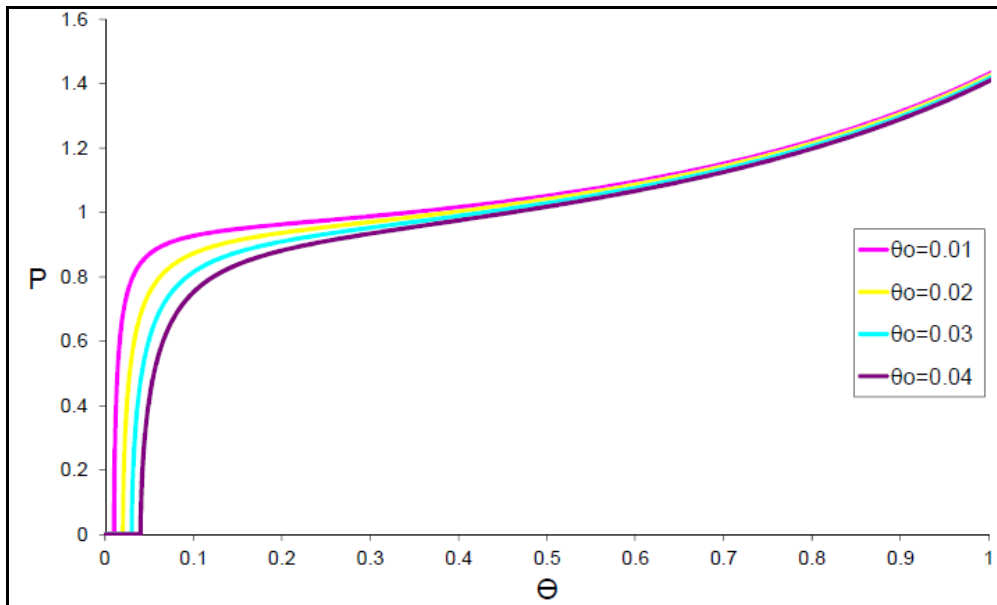


Figure 11. Post-Buckling Behaviour - Compression

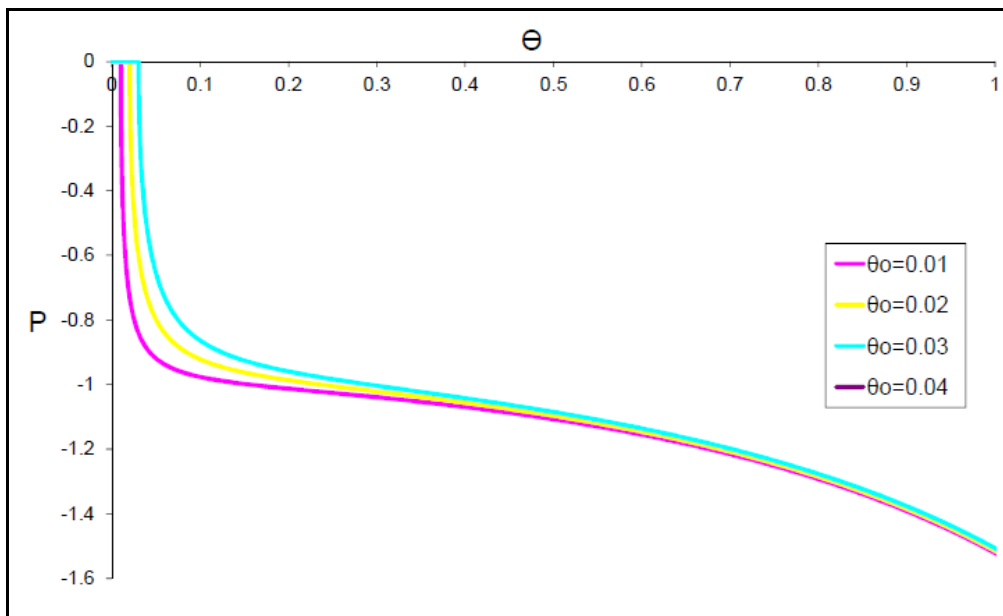


Figure 12. Post-Buckling Behaviour – Tensile

CONCLUSIONS

The study conducted in this paper may be viewed as a way to interpret the results of the linear theory of multi-layered elastomeric bearings and to extend it indicating that these items are stable in their post-buckling behaviour. By replacing the differential equations for the continuous model by the algebraic equations of the simple model, it is easy to evaluate the post-buckling behaviour and the interactions at large deformations for both compressive and tensile cases.

The simple two-spring model has been used to help understand the somewhat unexpected result that isolator can buckle in tension at a load close to that for buckling in compression. In particular, this behavior is really tensile and the isolator mechanism in tension is the mirror image of that of the isolator in compression. It also shown that for a particular value of the tensile load the isolator deformation is pure shear, something which does not happen in an isolator in compression. This result may be useful in practical applications since if elastomeric bearings are used in the seismic isolation of tall buildings in near-fault locations, the seismic code requirements can lead to situations where some bearings in an isolated system may be required to take some amount of tension and may need to be tested under lateral displacement and vertical tension.

REFERENCES

- Buckle, I., Nagarajaiah, S., and Ferrell, K. (2002). "Stability of elastomeric isolation bearings: Experimental study". *Journal of Structural Engineering*, 128(1), 3–11.
- Forcellini D, Kelly JM (2014) " Analysis of the large deformation stability of elastomeric bearings", *Journal of Engineering Mechanics*, ASCE, 10.1061 (ASCE) EM.1943-7889.0000729, 04014036: 1-10.
- Gent AN (1964) "Elastic stability of rubber compression springs", *Journal of Mechanical Engineering Science*. 6(4):318-326.
- Han, X., Warn, G., and Kasalanati, A., (2013) "Dynamic Stability Testing of Isolation Systems Composed of Elastomeric Bearings and Implications for Design." *Structures Congress 2013*, pp. 2140-2150.
- Haringx JA. (1948) "On highly compressible helical springs and rubber rods, and their application for vibration-free mountings", III. Philips Research Reports, 4:206-220.
- Kelly, J.M. (1997). Earthquake-Resistant Design with Rubber, 2nd ed., Springer-Verlag, London, England.
- Koh C.G. and Kelly J.M. (1986). "Effects of axial load on Elastomeric Isolation Bearings" Report N. UCB/EERC1986/12, Earthquake Engineering Research Center, University of California, Berkeley.
- Nagarajaiah, S., and Ferrell, K. (1999). "Stability of elastomeric seismic isolation bearings" *Journal of Structural Engineering*, 125(9), 946–954.
- Sanchez J., Masroor A., Mosqueda G. and Ryan K. (2013) "Static and Dynamic Stability of Elastomeric Bearings for Seismic Protection of Structures", *Journal of Structural Engineering* 139, SPECIAL ISSUE: NEES 1: Advances in Earthquake Engineering, 1149–1159. Technical Papers.
- Warn, G and Weisman, J (2011). "Parametric finite element investigation of the critical load capacity of elastomeric strip bearings". *Engineering Structures*, 33:12, 3509-3515.
- Weisman, J. and Warn, G., (2012). "Stability of Elastomeric and Lead-Rubber Seismic Isolation Bearings." *Journal of Structural Engineering*, 138:2, 215-223.